

The Nuclear EoS: from experiments to astrophysical observations

Isaac Vidaña, INFN Catania



**QFC2022 – Quantum gases,
Fundamental Interactions &
Cosmology
Pisa (Italy), October 26th-28th 2022**



In this talk ...

I will review different experimental and astrophysical observational (NSs) constraints of the nuclear EoS (*i.e.*, thermodynamical relation between pressure & energy density $P=P(\epsilon)$) as well as some of the ab-initio theoretical many-body approaches & phenomenological models commonly used in its description

Three recent reviews on the topic are



M. Oertel, M. Hempel, T. Klahn & S. Typel, Rev. Mod. Phys. 89, 015007 (2017)



F. Burgio & A. Fantina, in “The Physics & Astrophysics of Neutron Stars”, L. Rezzolla, P. Pizzochero, I. Jones, N. Rea & I.V. Eds, Springer-Verlag 2018



F. Burgio, H.-J. Schulze, I.V. & J. B. Wei, Prog. Part. Nucl. Phys. 120, 103879 (2021)

The Nuclear EoS

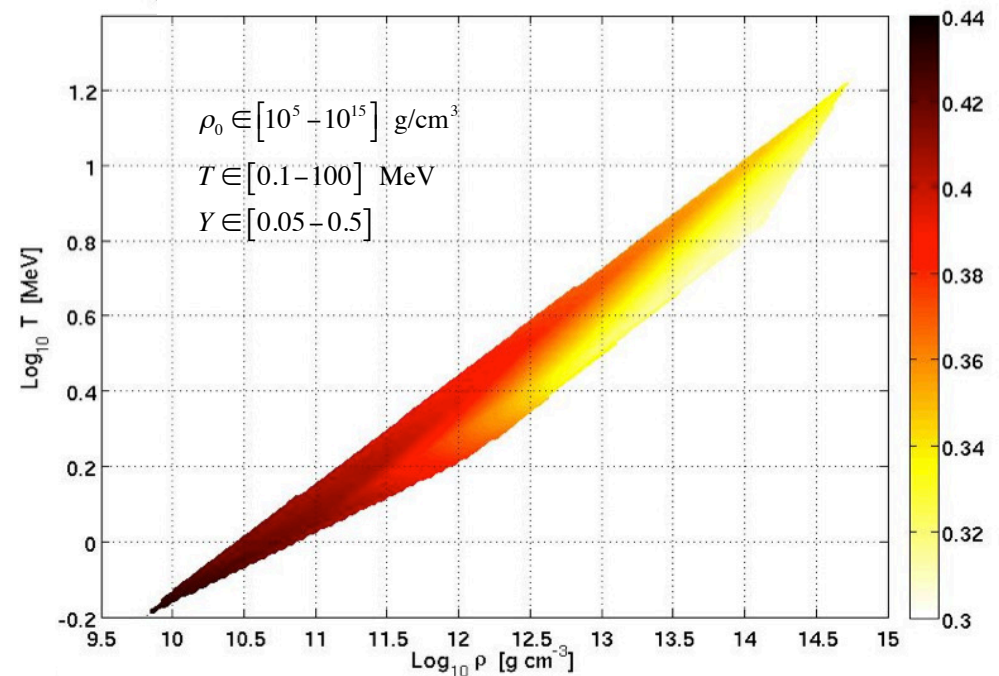
The Nuclear EoS is a fundamental ingredient for the understanding of the static & dynamical properties of NS, core-collapse SN & compact star mergers

However, its determination is **very challenging** due to the **wide range of densities, temperatures & isospin asymmetries** found in these astrophysical scenarios.

Main **difficulties** associated to:

- ✓ Complexity of the **bare baryon-baryon interaction**
- ✓ Very **complicated resolution** of the so-called **nuclear many-body problem**

Conditions in the center of the star from the onset of the collapse up to 25 ms after bounce ($15 M_{\text{sun}}$ progenitor)

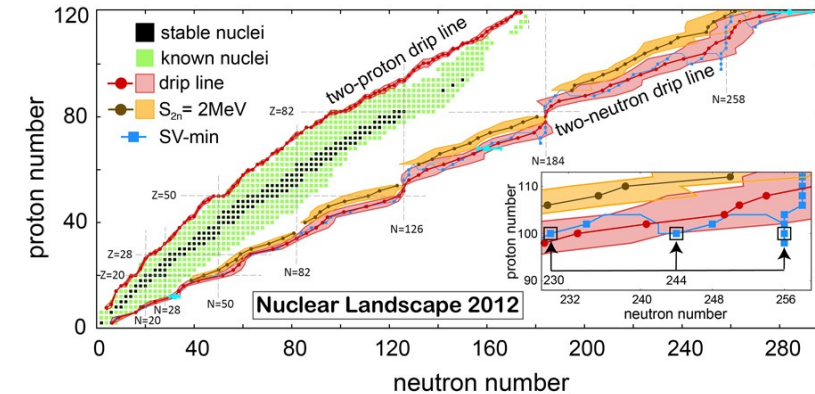


What do we know to build the nuclear EoS ?



J. Erler et al., Nature 486, 509 (2012)

- ✧ Masses, radii & other properties of more than 3000 isotopes
- ✧ Scattering (cf. > 4000 NN data for $E_{\text{lab}} < 350$ MeV)

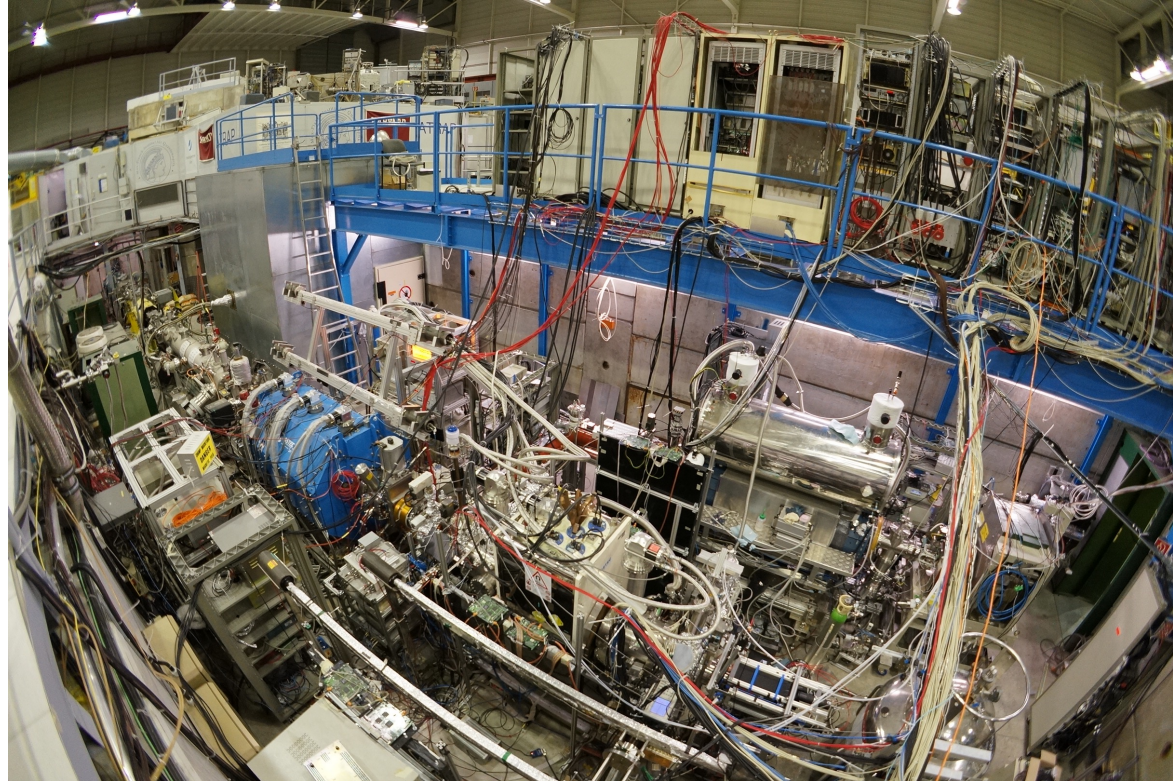


- Around ρ_0 & $\beta=0$ the nuclear EoS can be characterized by a few **isoscalar** (E_0, K_0, Q_0) & **isovector** ($E_{\text{sym}}, K_{\text{sym}}, Q_{\text{sym}}$) parameters which can be constrained by **nuclear experiments** & **astrophysical observables**

$$\frac{E}{A}(\rho, \beta) = E_0 + \frac{1}{2}K_0x^2 + \frac{1}{6}Q_0x^3 + \left(E_{\text{sym}} + Lx + \frac{1}{2}K_{\text{sym}}x^2 + \frac{1}{6}Q_{\text{sym}}x^3 \right) \beta^2 + \dots, \quad x = \frac{\rho - \rho_0}{3\rho_0}$$

- **Extrapolation to high densities** should rely on **theoretical models** to be tested with **astrophysical observations**

Constraints from Nuclear Physics Experiments



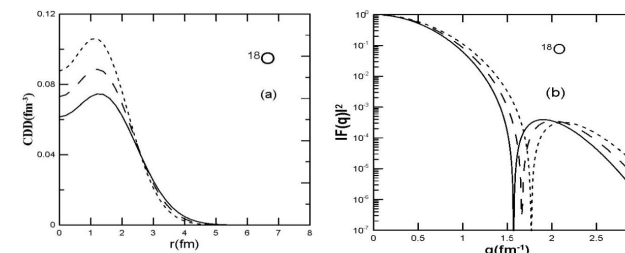
Density Distributions & Nuclear Binding Energies

✧ Density distributions:

(e,e') elastic scattering, hadron probes

$$A = N + Z \rightarrow \infty$$

$$\rho_0 \sim 0.16 \text{ fm}^{-3}$$



✧ Nuclear binding energies:

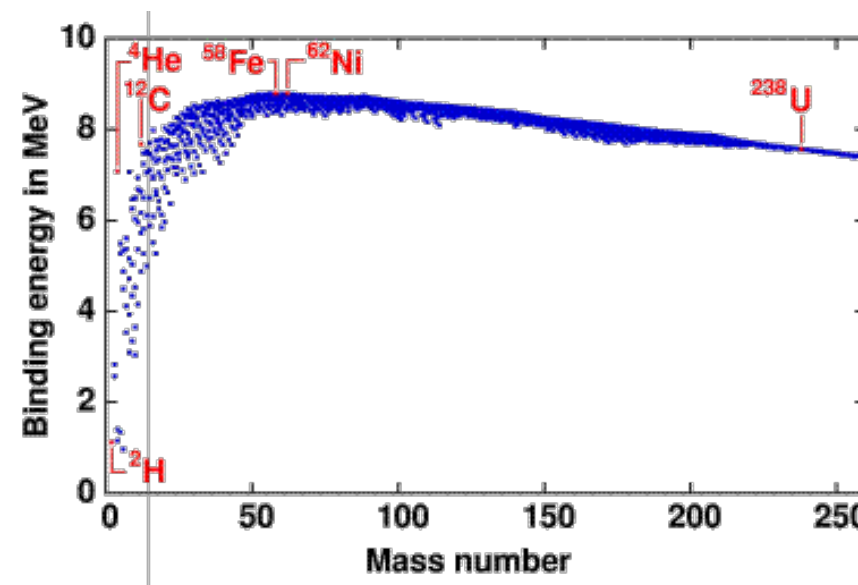
$$B(N, Z) = a_v A + a_s A^{2/3} + a_c \frac{Z^2}{A^{1/3}} + (a_{Av} A + a_{As} A^{2/3}) \frac{(N - Z)^2}{A^2} + \delta a_p A^{-1/2}$$

Measurements of nuclear binding energies allow the identification

$$a_v \Leftrightarrow B_{sat} = -E_0$$

$$a_{Av} \Leftrightarrow E_{sym}$$

(in the limit $A = N + Z \rightarrow \infty$)



Recent **fits** of binding energies with **non-relativistic** & **relativistic** EDF give

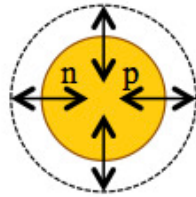
SHF models: $B_{sat} = (15.96 \pm 0.31) \text{ MeV}$, $E_{sym} = (31.2 \pm 6.7) \text{ MeV}$

RMF models: $B_{sat} = (16.13 \pm 0.51) \text{ MeV}$, $E_{sym} = (33.4 \pm 4.7) \text{ MeV}$



Nuclear Resonances

✧ ISGMR



$$\Delta L=0$$

$$\Delta S=0, \Delta T=0$$

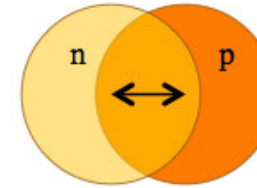
Collective monopole mode oscillation of all **neutrons & protons** in a nucleus vibrating **in phase**

K_0 from the measurement of **excitation energy** E_{ISGMR}
Typical values in the range $\sim 210 - 270$ MeV



Phys. Rep. 64, 171 (1980); PRC 90, 055203 (2014)

✧ IVGDR



$$\Delta L=1$$

$$\Delta S=0, \Delta T=1$$

Collective dipole model oscillation of all **neutrons & protons** in a nucleus vibrating **in opposite phase**

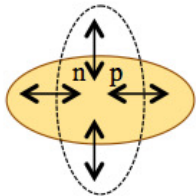
Symmetry energy influences the **excitation energies** of IVGDR. Their analysis allows to determine E_{sym}

$$23.3 < E_{\text{sym}}(\rho = 0.1 \text{ fm}^{-3}) = 24.9 \text{ MeV}$$



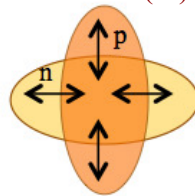
Trippa et al., PRC 77, 061304 (R) (2008)

✧ ISGQR & IVGQR



$$\Delta L=2$$

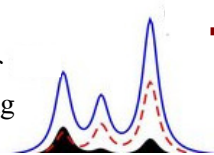
$$\Delta S=0, \Delta T=0$$



$$\Delta L=2$$

$$\Delta S=0, \Delta T=1$$

Collective quadrupole mode oscillation of all **neutrons & protons** in a nucleus vibrating **in (IS) & out (IV) of phase**



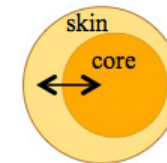
Correlation of Δr_{np} with **ISGQR & IVGQR** **excitation energies** from which

$$\Delta(^{208}\text{Pb}) = 0.14 \pm 0.03 \text{ fm}, \quad L = 37 \pm 18 \text{ MeV}$$



Roca-Maza et al., PRC 87, 037301 (2013)

✧ PDR



Collective oscillation of **neutron skin** against the **core**

Sensitive to the **symmetry energy**. A recent analysis of PDR in ^{68}Ni & ^{132}Sn using RPA models for the dipole response based in Skyrme & RMF give

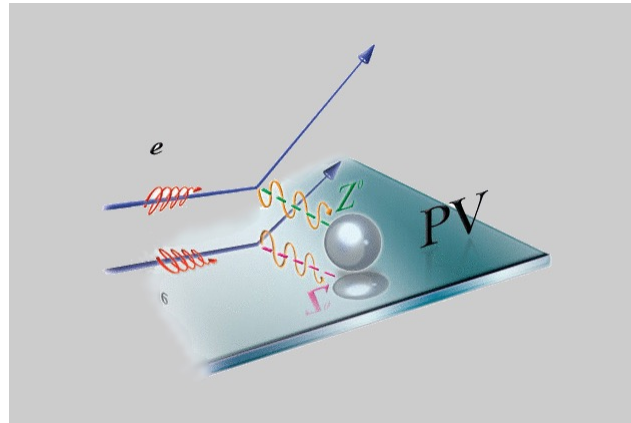
$$E_{\text{sym}} = 32.3 \pm 1.3 \text{ MeV}, \quad L = 64.8 \pm 15.7 \text{ MeV}$$



Carbone et al., PRC 81, 041301 (R) (2010)

Neutron Skin Thickness & Symmetry Energy

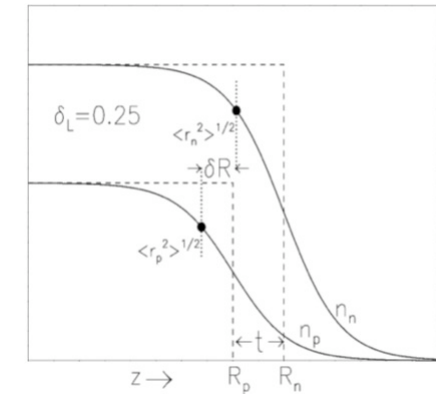
Accurate measurements of Δr_{np} via **parity-violating electron scattering** at JLAB can constrain $E_{\text{sym}}(\rho)$, particularly **L** via its **strong correlation** with Δr_{np}



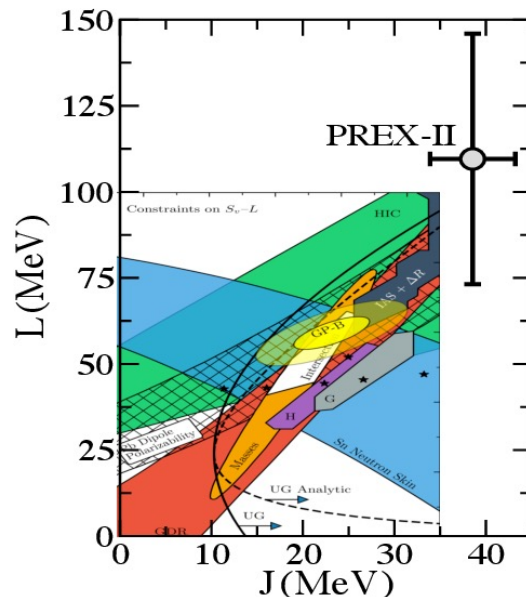
neutron form factor

$$A_{pv} = \frac{\sigma_{\uparrow} - \sigma_{\downarrow}}{\sigma_{\uparrow} + \sigma_{\downarrow}} \approx \frac{G_F q^2}{4\pi\alpha\sqrt{2}} \frac{F_n(q)}{F_p(q)}$$

proton form factor



$$\Delta r_{np} = \sqrt{\langle r_n \rangle^2} - \sqrt{\langle r_p \rangle^2}$$



CREX & PREX-II experiments

$$\Delta r_{np}(^{48}\text{Ca}) = 0.121 \pm 0.026 \text{ fm}$$

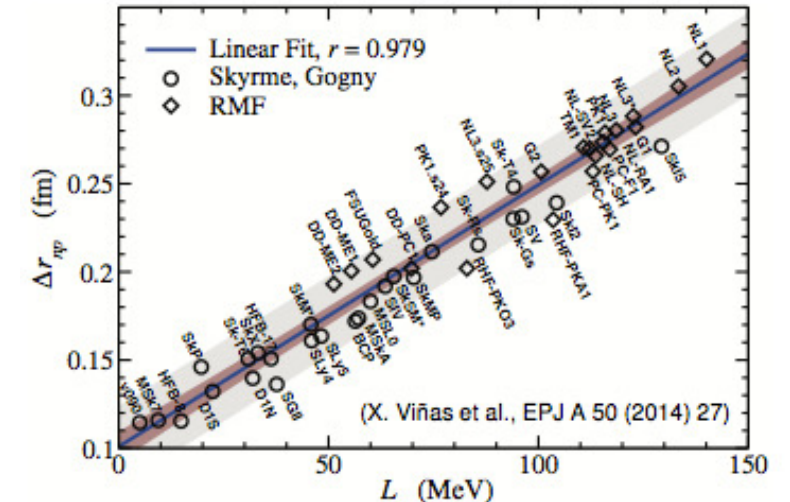
$$\Delta r_{np}(^{208}\text{Pb}) = 0.283 \pm 0.071 \text{ fm}$$

$$E_{\text{sym}} = 34-42 \text{ MeV}$$

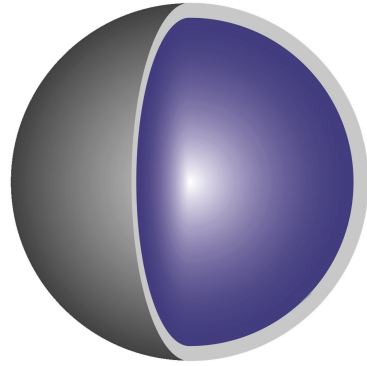
$$L = 74-149 \text{ MeV}$$



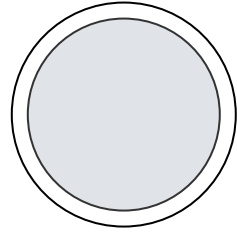
PRL 126, 172502 (2021)



Neutron Skin Thickness & Crust-Core Transition Density in Neutron Stars



Neutron Star



Heavy nucleus

Neutron Star Crust & Neutron Skin are made out of neutron rich matter at similar densities

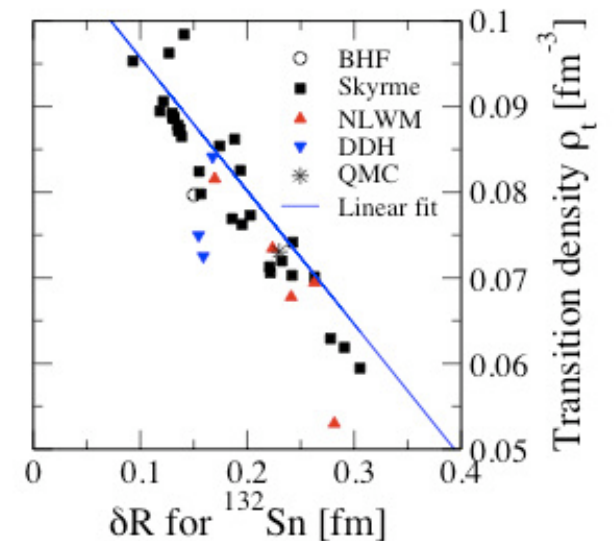
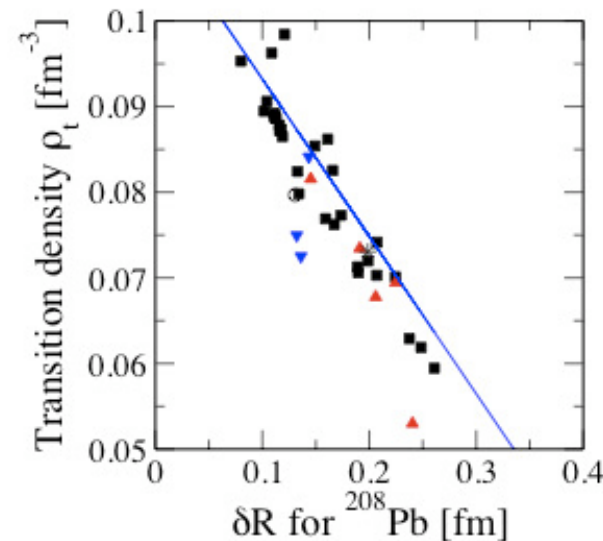


Both are governed by EoS at subnuclear densities in particular by $E_{\text{sym}}(\rho)$ & its derivatives

Inverse correlation between δR and ρ_t
(Horowitz & Piekarewicz)



Accurate measurements of neutron skin in neutron rich nuclei such as the ones performed at JLAB can provide considerable & valuable information on the crust-core transition density



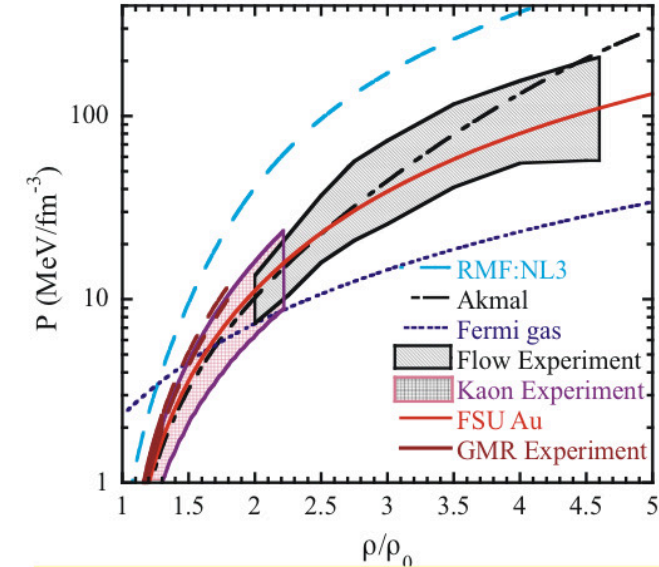
EoS from Heavy Ion Collisions

The analysis of data from HIC requires the use of **transport models** which **do not depend directly on the EoS** but rather on the **mean field** of the participant particles & the **in-medium cross sections** of the relevant reactions

However, there are several transport codes in the market. A natural question arises: **How much the results depend on the transport codes ?**



P. Danielewicz et al., Science 298, 1592 (2002)



Several observables in HIC are sensitive to the nuclear EoS

sub-saturation densities

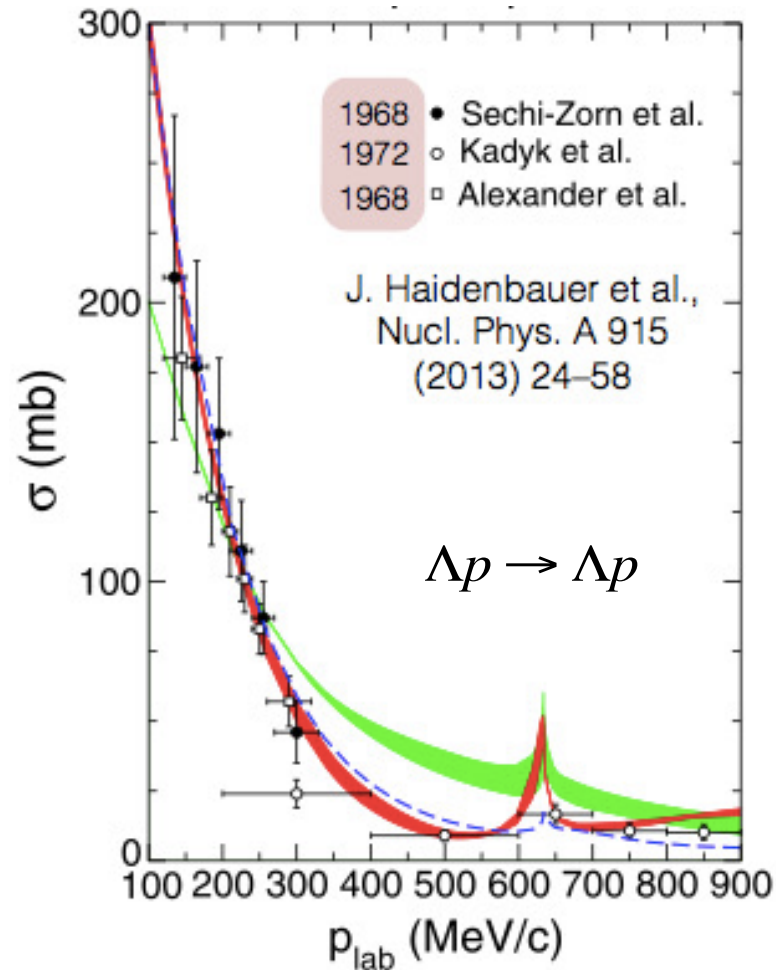
- ✓ n/p & $t^3\text{He}$ ratios
- ✓ isospin fragmentation & isospin scaling
- ✓ np correlation functions at low rel. mom.
- ✓ isospin diffusion/transport
- ✓ neutron-proton differential flow

supra-saturation densities

- ✓ π^-/π^+ & K^-/K^+ ratios
- ✓ np differential transverse flow
- ✓ nucleon elliptic flow at high trans. mom.
- ✓ n/p ratio of squeezed out nucleons perpendicular to the reaction plane

What do we know to include hyperons in the nuclear EoS ?

Hyperons are expected to appear in the interior of NSs and play an important role on their structure & properties, however, our knowledge of the YN & YY interactions is much more limited than that on the NN one in order to put to put stringent constraints on hypernuclear EoS



➤ Very few YN scattering data due to short lifetime of hyperons & low intensity beam fluxes

- ~ 35 data points, all from the 1960s
- 10 new data points, from KEK-PS E251 collaboration (2000)

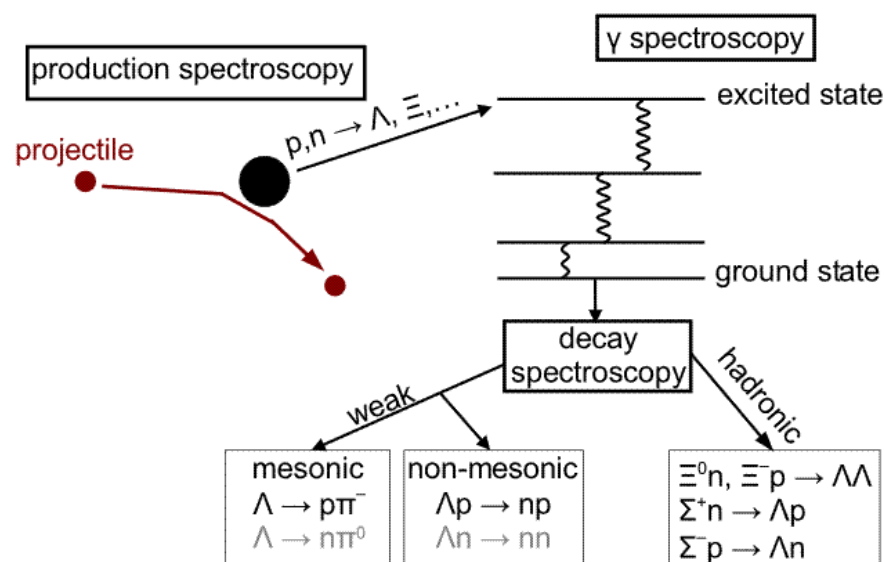
➤ No YY scattering data exists

(cf. > 4000 NN data for $E_{\text{lab}} < 350$ MeV)

Hypernuclear Physics in a Nutshell

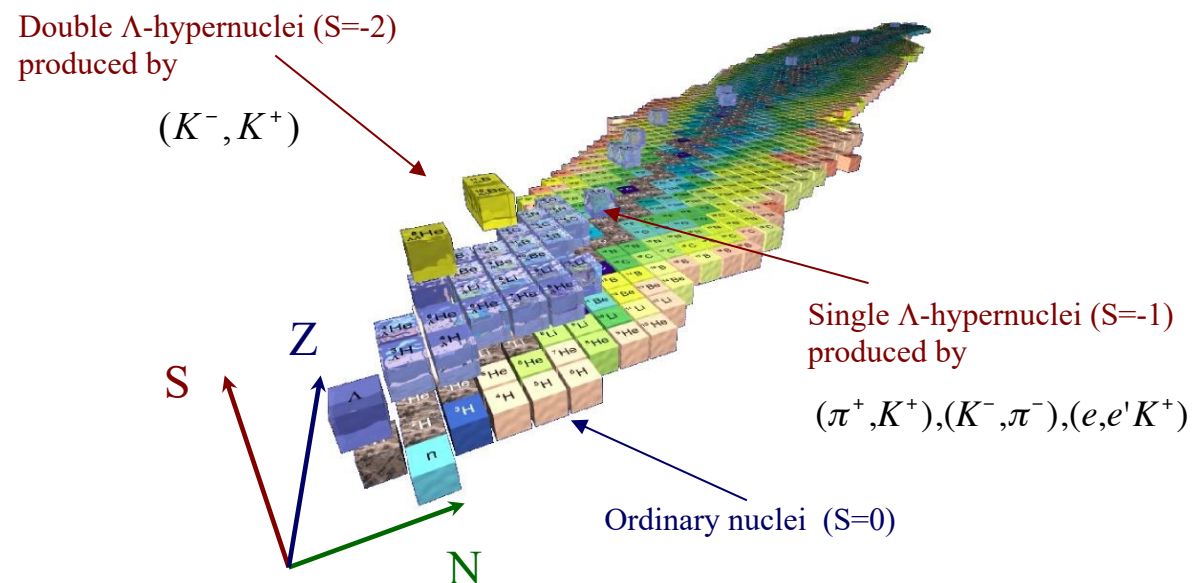


Alternative information can be obtained from the study of **hypernuclei** (bound nuclear systems of nucleons & hyperons). The **goal of hypernuclear physics** is to relate hypernuclear observables with the underlying bare YN & YY interactions



- 41 single Λ -hypernuclei \rightarrow ΛN attractive ($U_{\Lambda}(\rho_0) \sim -30$ MeV)
- 3 double- Λ hypernuclei \rightarrow weak $\Lambda\Lambda$ attraction ($\Delta B_{\Lambda\Lambda} \sim 1$ MeV)
- Very few Ξ -hypernuclei \rightarrow ΞN attractive ($U_{\Xi}(\rho_0) \sim -14$ MeV)
- Ambiguous evidence of Σ -hypernuclei \rightarrow ΣN repulsive ($U_{\Sigma}(\rho_0) > +15$ MeV) ?

- Strangeness exchange production: ${}^A Z (K^-, \pi^-) {}^A_{\Lambda} Z$
- Associate strangeness production: ${}^A Z (\pi^+, K^-) {}^A_{\Lambda} Z$
- Electroproduction: ${}^A Z (e' K^+) {}^A_{\Lambda} (Z - 1)$
- Production in HIC



Astrophysical (Neutron Stars) Constraints



Neutron Star Masses

NS masses can be inferred directly from
observations of binary systems

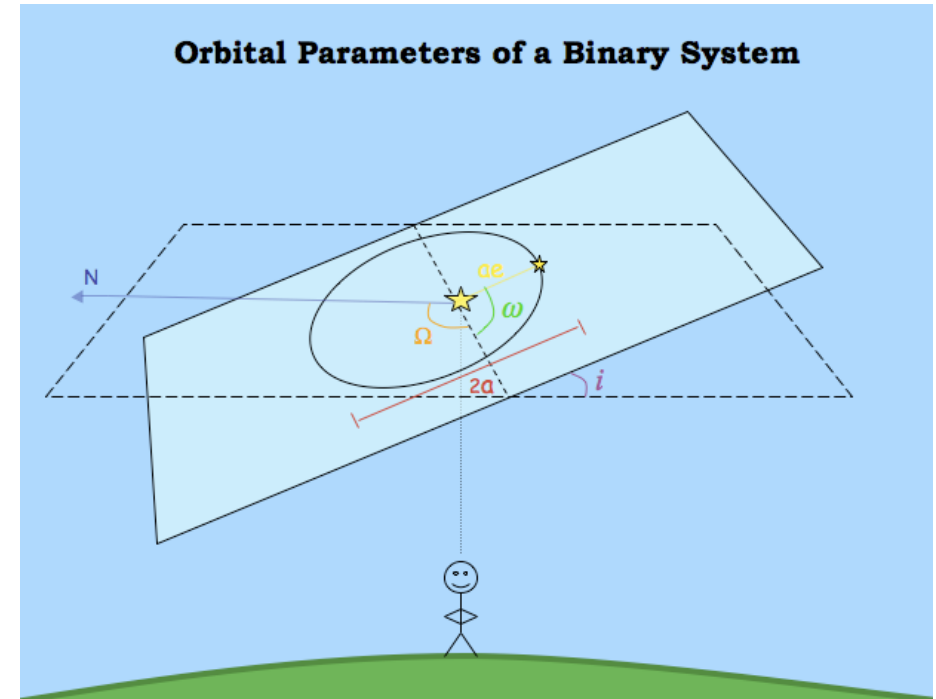
- 5 orbital (Keplerian) parameters can be precisely measured:
 - ✓ Orbital period (P)
 - ✓ Projection of semimajor axis on line of sight ($a \sin i$)
 - ✓ Orbit eccentricity (ϵ)
 - ✓ Time of periastron (T_0)
 - ✓ Longitude of periastron (ω_0)
- 3 unknowns: M_1, M_2, i

Kepler's 3rd law

$$\frac{G(M_1 + M_2)}{a^3} = \left(\frac{2\pi}{P} \right)^2 \rightarrow$$

$$f(M_1, M_2, i) \equiv \frac{(M_2 \sin i)^3}{(M_1 + M_2)^2} = \frac{Pv^3}{2\pi G}$$

mass function



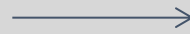
In few cases small deviations from Keplerian orbit due to GR effects can be detected

Measure of at least 2 post-Keplerian parameters



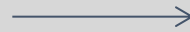
High precision NS mass determination

$$\dot{\omega} = 3T_{\otimes}^{2/3} \left(\frac{P_b}{2\pi} \right)^{-5/3} \frac{1}{1-\varepsilon} (M_p + M_c)^{2/3}$$



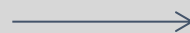
Advance of the periastron

$$\gamma = T_{\otimes}^{2/3} \left(\frac{P_b}{2\pi} \right)^{1/3} \varepsilon \frac{M_c (M_p + 2M_c)}{(M_p + M_c)^{4/3}}$$



Time dilation & grav. redshift

$$r = T_{\otimes} M_c$$



Shapiro delay “range”

$$s = \sin i = T_{\otimes}^{-1/3} \left(\frac{P_b}{2\pi} \right)^{-2/3} x \frac{(M_p + M_c)^{2/3}}{M_c}$$



Shapiro delay “shape”

$$\dot{P}_b = -\frac{192\pi}{5} T_{\otimes}^{5/3} \left(\frac{P_b}{2\pi} \right)^{-5/3} f(\varepsilon) \frac{M_p M_c}{(M_p + M_c)^{1/3}}$$



Orbit decay due to GW emission

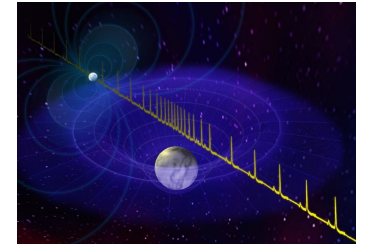
Recent Measurements of High NS Masses

■ PSR J164-2230 (Demorest et al. 2010)

- ✓ binary system ($P=8.68$ d)
- ✓ low eccentricity ($\varepsilon=1.3 \times 10^{-6}$)
- ✓ companion mass: $\sim 0.5M_{\odot}$
- ✓ pulsar mass: $M = 1.928 \pm 0.017M_{\odot}$

In this decade NS with $2M_{\odot}$ have been observed by measuring **Post-Keplerian parameters** of their orbits

- Advance of the periastron $\dot{\omega}$
- **Shapiro delay** (range & shape)
- Orbital decay \dot{P}_b
- Grav. redshift & time dilation γ



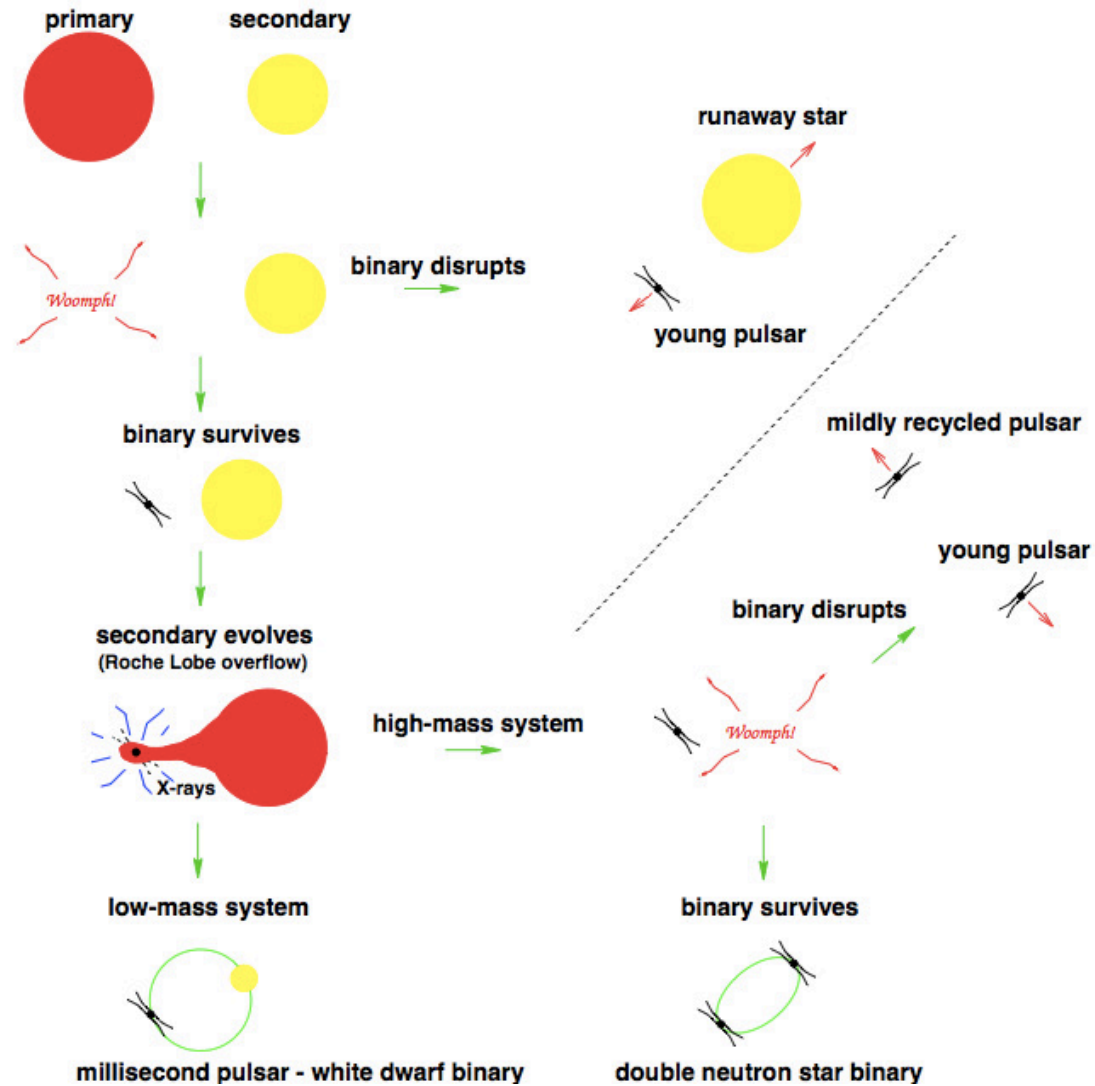
■ PSR J0348+0432 (Antoniadis et al. 2013)

- ✓ binary system ($P=2.46$ h)
- ✓ very low eccentricity
- ✓ companion mass: $0.172 \pm 0.003M_{\odot}$
- ✓ pulsar mass: $M = 2.01 \pm 0.04M_{\odot}$

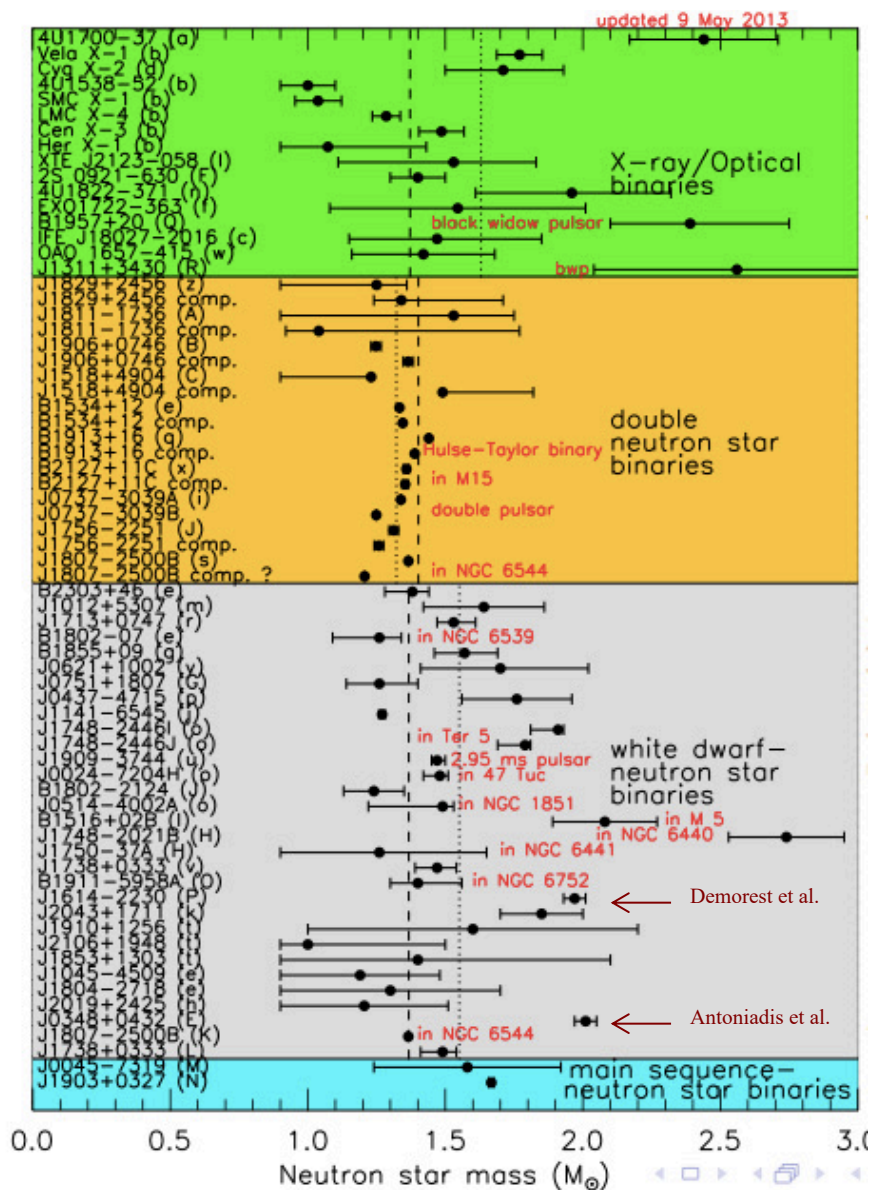
■ MSP J0740+6620 (Cromartie et al. 2020)

- ✓ binary system ($P=4.76$ d)
- ✓ low eccentricity ($\varepsilon=5.10(3) \times 10^{-6}$)
- ✓ companion mass: $0.258(8)M_{\odot}$
- ✓ pulsar mass: $M = 2.14^{+0.10}_{-0.09}M_{\odot}$ (68.3% c.i.)
 $M = 2.14^{+0.20}_{-0.018}M_{\odot}$ (95.4% c.i.)

Formation of Binary Systems



Measured Neutron Star Masses (2022)



Observation of $\sim 2 M_{\odot}$ neutron stars imposes a very stringent constraint



Any reliable nuclear EoS should satisfy

$$M_{\max} [EoS] > 2 M_{\odot}$$

otherwise is rule out

updated from Lattimer 2013

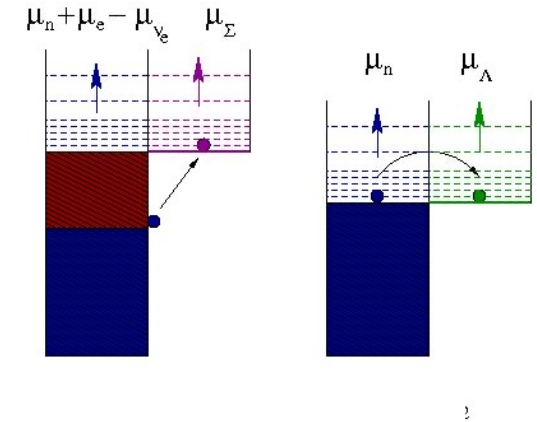
The Hyperon Puzzle



Hyperons are expected to appear in the core of neutron stars at $\rho \sim (2-3)\rho_0$ when μ_N is large enough to make the **conversion of N into Y energetically favorable**

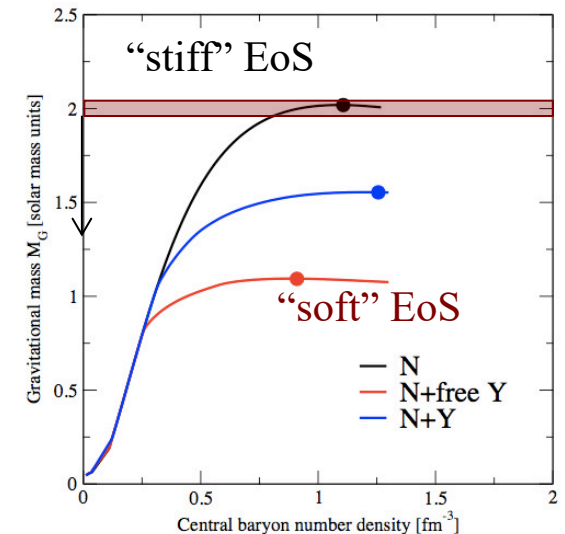
But

The relieve of Fermi pressure due to its appearance leads to a **softer EoS** and, therefore, to a **reduction of the mass** to values incompatible with observation



Observation of $\sim 2 M_{\odot}$ NS \longrightarrow Any reliable EoS of dense matter should predict $M_{\max}[EoS] > 2 M_{\odot}$

Can hyperons be present in the interior of neutron stars in view of this stringent constraint ?



Limits on the Neutron Star Radius

The radius of a neutron star with mass M **cannot be arbitrarily small**

General Relativity:
a Neutron Star is not a
Black Hole

$$R > \frac{2GM}{c^2}$$

Finite Pressure:
Neutron Star matter cannot
be arbitrarily compressed

$$R > \frac{9}{4} \frac{GM}{c^2}$$

Causality:
speed of sound must
be smaller than c

$$R > 2.9 \frac{GM}{c^2}$$

The desired measurement of neutron star radii

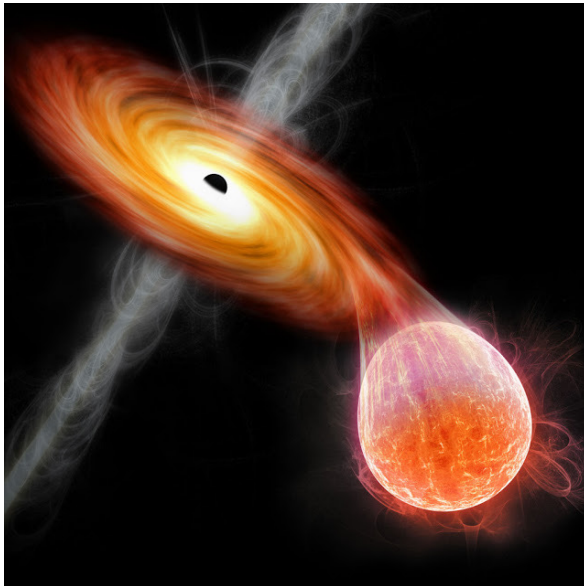
Radii are **very difficult to measure** because NS:

- ✧ are **very small** (~ 10 km)
- ✧ are **far from us** (e.g., the closest NS, RX J185635-3754, is at ~ 200 ly, moving at 100 km/s)



Credit by NASA

A possible way to measure it is to use the **thermal emission of low mass X-ray binaries**:



NS radius can be obtained from:

- ✧ **Flux measurement** + Stefan-Boltzmann's law
- ✧ **Temperature** (Black body fit + atmosphere model)
- ✧ **Distance estimation** (difficult)
- ✧ **Gravitational redshift z** (detection of absorption lines)

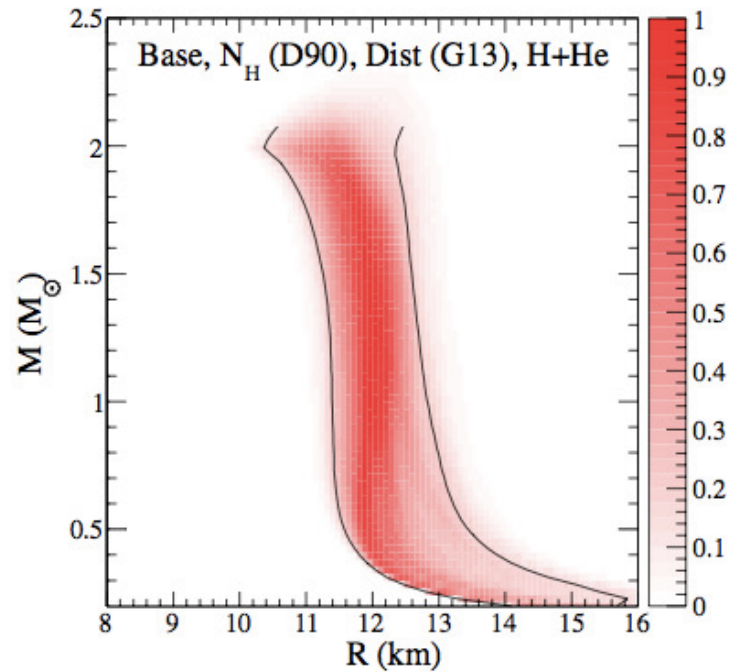
$$R_{\infty} = \sqrt{\frac{FD^2}{\sigma_{SB}T^4}} \rightarrow R_{NS} = \frac{R_{\infty}}{1+z} = R_{\infty} \sqrt{1 - \frac{2GM}{R_{NS}c^2}}$$

Estimations of Neutron Star Radii from LMXB

The conclusion from past analysis of the thermal spectrum from 5 quiescent LMXB in globular clusters **was controversial**



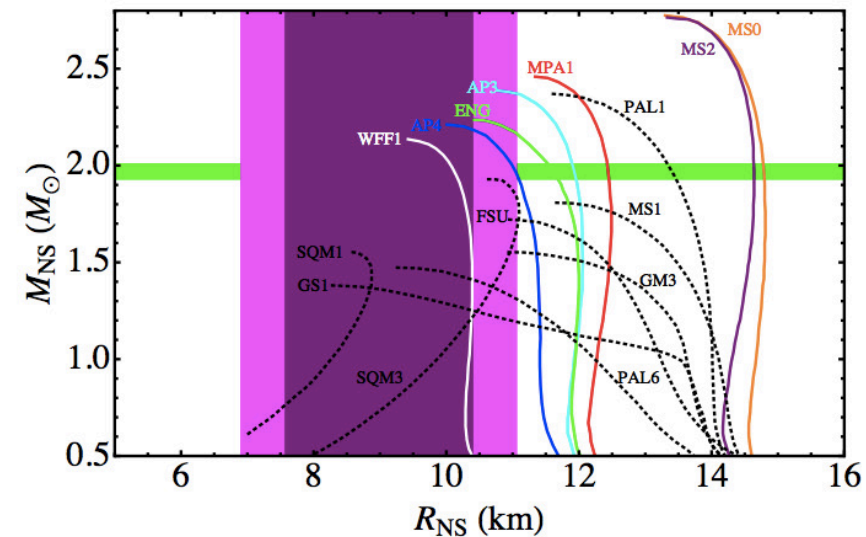
Steiner et al. (2013, 2014)



$$R = 12.0 \pm 1.4 \text{ km}$$



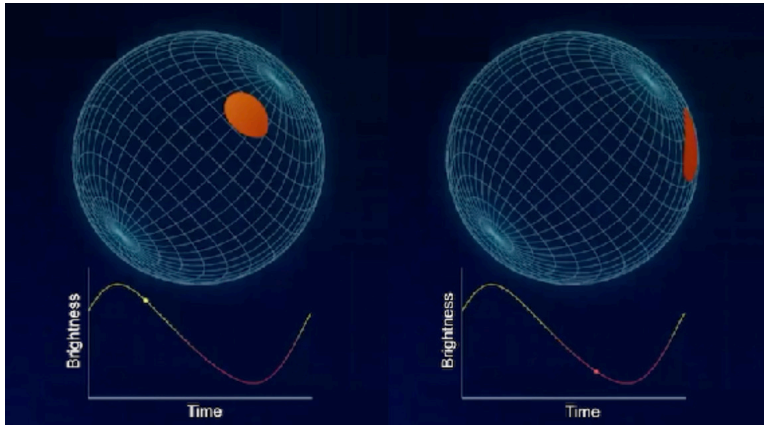
Guillot et al. (2013, 2014)



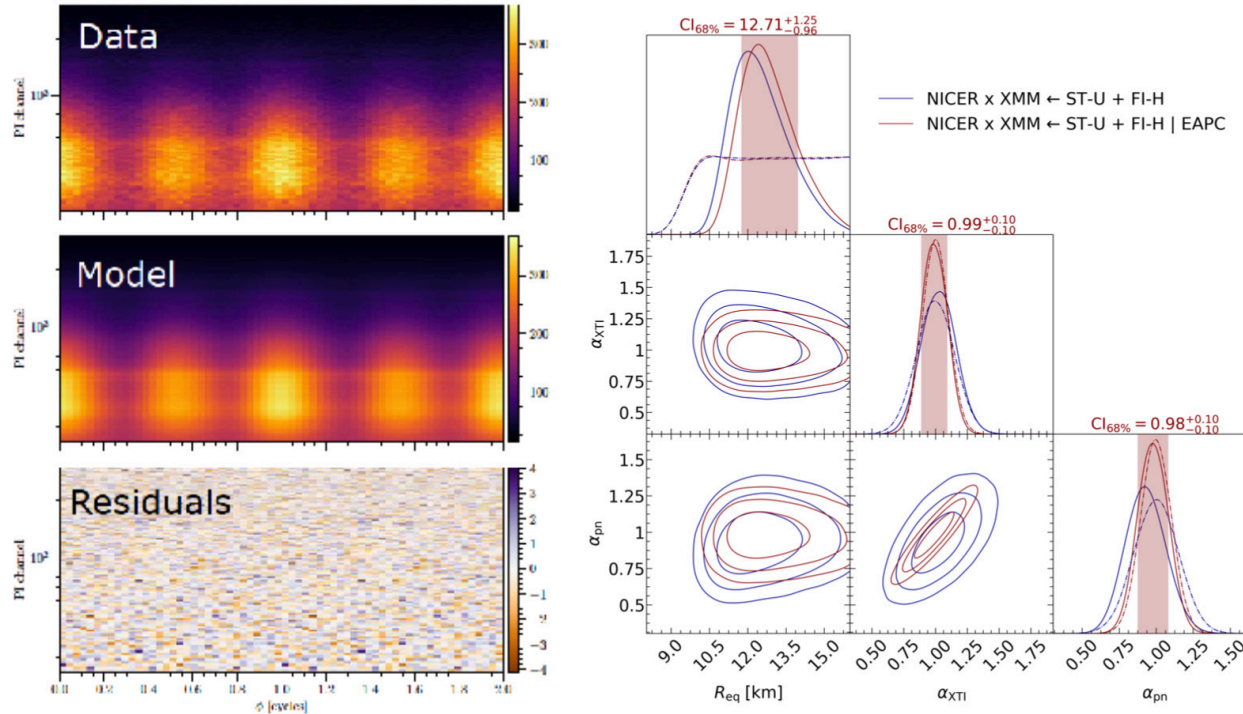
$$R = 9.1^{+1.3}_{-1.5} \text{ km} \text{ 2013 analysis}$$

$$R = 9.4 \pm 1.2 \text{ km} \text{ 2014 analysis}$$

NICER: Neutron Star Interior Composition Explorer



A new way of measuring NS radius by tracking the X-ray emission from “hot spots” on the star’s surface as the star rotates. M/R is extracted by modeling the Pulse Profile of the hot spots



✧ PSR J0740+6620

$$M = 2.072^{+0.067}_{-0.066} M_{\odot}$$

$$R = 13.7^{+2.6}_{-1.5} \text{ km} \quad \text{Miller et al., arXiv:2105.06979}$$

$$R = 12.39^{+1.30}_{-0.98} \text{ km} \quad \text{Riley et al., arXiv:2105.06980}$$

✧ PSR J0030+0451

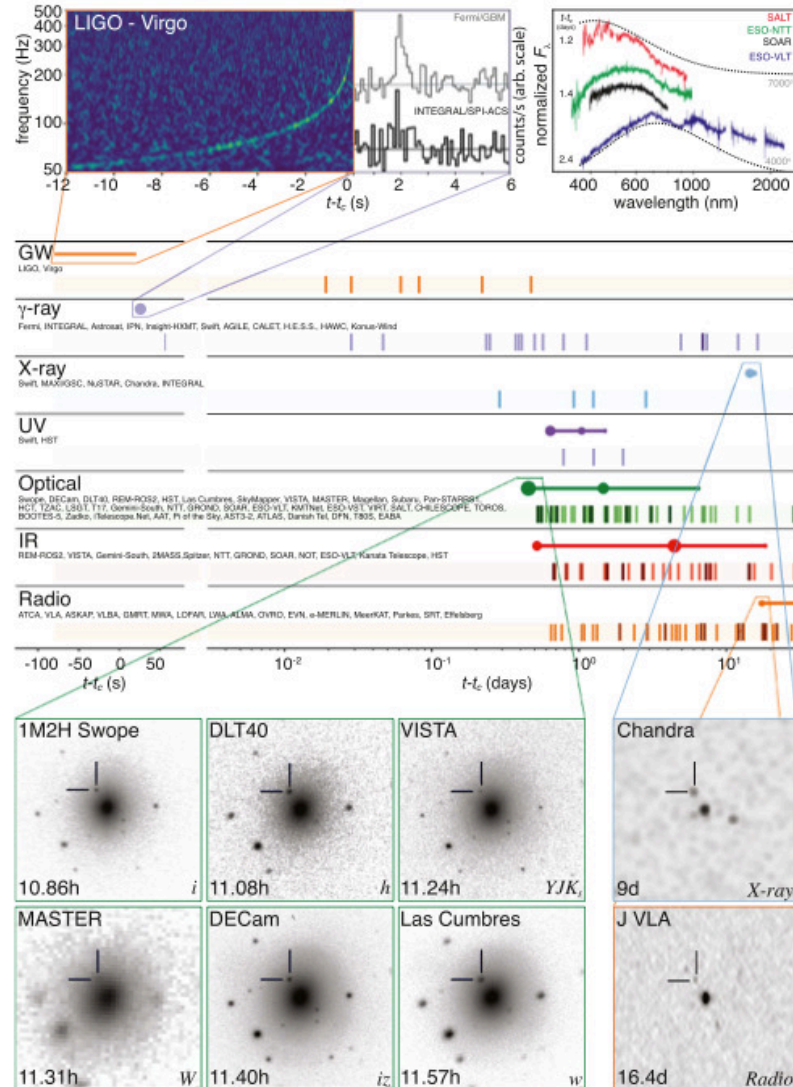
$$M/R = 0.156^{+0.008}_{-0.010}$$

$$R = 13.02^{+1.24}_{-1.06} \text{ km} \quad \text{Miller et al., ApJ 887 L24 (2019)}$$

$$R = 12.71^{+1.14}_{-1.19} \text{ km} \quad \text{Riley et al., APJ 887 L21 (2019)}$$

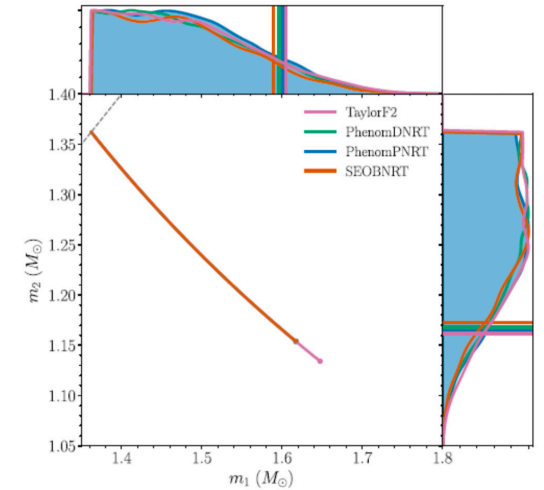
GW170817: the first NS-NS merger

Multi-messenger observations of the event GW170817



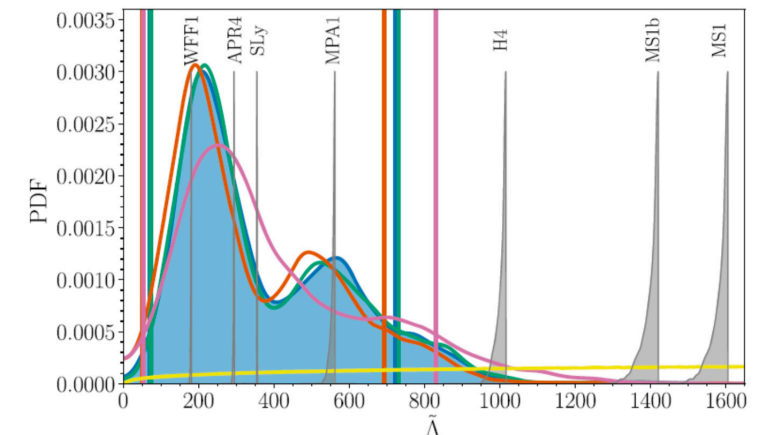
✧ Masses estimated from the **chirp mass**

$$M_c = \frac{(m_1 m_2)^{3/5}}{(m_1 + m_2)^{1/5}}$$



✧ Radius from the **tidal deformability**

$$\tilde{\Lambda} = \frac{16}{13} \frac{(1+12q)\Lambda_1 + (q+12)\Lambda_2}{(1+q)^5}$$



A $1.36M_{\odot}$ has a radius of 10.4 km (WFF1), 11.3 km (APR4), 11.7 km (Sly), 12.4 km (MPA1), 14.0 (H4), 14.5 (MS1b) and 14.9 km (MS1)

Thermal Evolution of Neutron Stars

Information, complementary to that from mass & radius, can be also obtained from the measurement of the **temperature (luminosity) of neutron stars**

Two cooling regimes

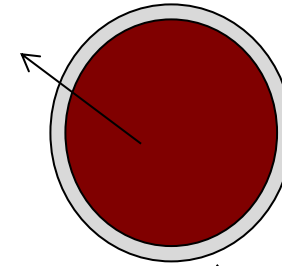
Slow

Low NS mass

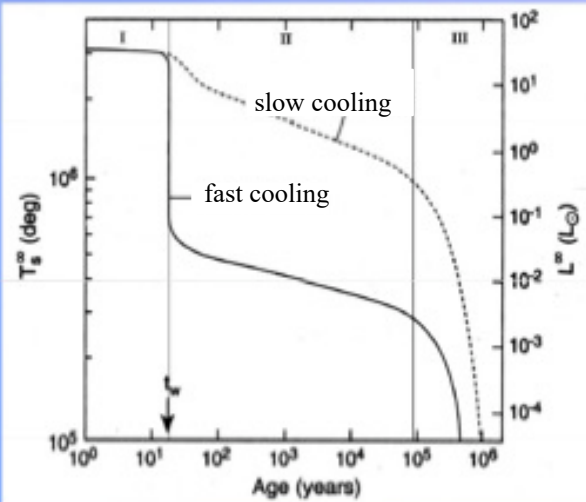
Fast

High NS mass

Core cools by
neutrino emission



Surface photon emission
dominates at $t > 10^6$ yrs



- I. Core relaxation epoch
- II. Neutrino cooling epoch
- III. Photon cooling epoch

$$\frac{dE_{th}}{dt} = C_v \frac{dT}{dt} = -L_\gamma - L_\nu + H$$

✓ C_v : specific heat

✓ L_γ : photon luminosity

✓ L_ν : neutrino luminosity

✓ H : “heating”

Strong dependence on the NS
composition & EoS

Other neutron star observables

Other **NS observables** can also help to constraint direct or indirectly the nuclear EoS

✧ Gravitational Redshift:

$$z = \left(1 - \frac{2GM}{c^2 R}\right)^{-1/2} - 1$$

Measurements of z allow to **constraint the ratio of M/R**

✧ Quasi-periodic Oscillations:

QPO in X-ray binaries measure the difference between the NS rot. freq. & the Keplerian freq. of the innermost stable orbit of matter elements in the accretion disk. Their observation & analysis can put **stringent constraints on masses, radii & rotational periods**

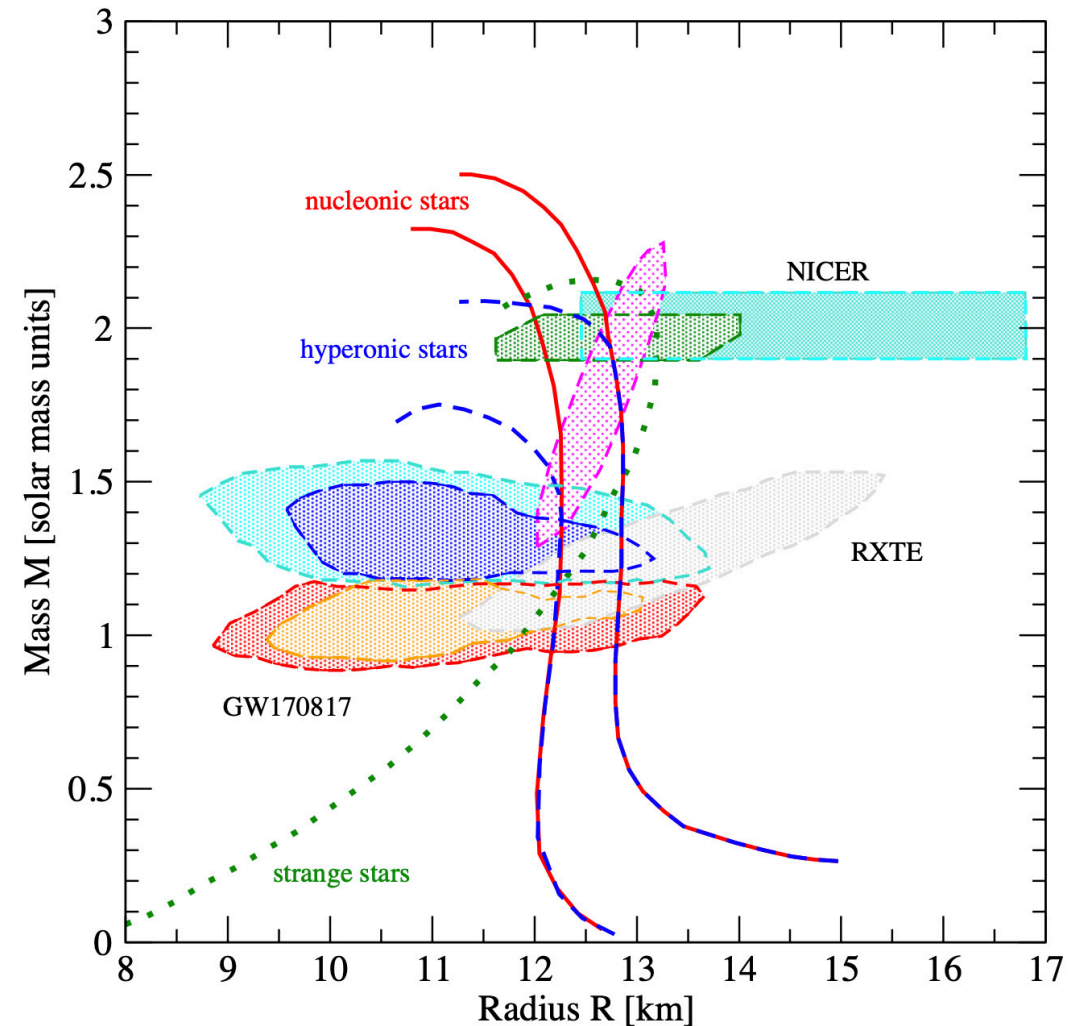
✧ NS moment of inertia:

$$I = \frac{J(\Omega)}{\Omega}; \quad J(\Omega) = \frac{8\pi}{3} \int_0^R dr r^4 \frac{p(r) + \varepsilon(r)}{\sqrt{1 - \frac{2M(r)}{r}}} (\Omega - \omega(r)) e^{-\nu(r)}$$

Measurements of I could also **constraint EoS**. But **not measured yet**. Lower bound can be inferred from timing observations of Crab pulsar

Combined analysis of a few astrophysical data

- ✧ NICER PSR J0740+6620 & PSR J0030+0451
- ✧ GW170817
- ✧ Rossi X-ray Timing Explorer (RXTE) results for the cooling tail spectra of 4U1702-429



Building the Nuclear EoS



Approaches to the Nuclear EoS: “Story of Two Philosophies”

Ab-initio Approaches

Based on two- & three-nucleon realistic interactions which reproduce scattering data & the deuteron properties. The EoS is obtained by “solving” the complicated many-body problem

- ✧ Variational approaches: FHNC
- ✧ Diagrammatic: methods: BBG (BHF), SCGF
- ✧ Monte-Carlo techniques: VMC, DMC, GMC, AFDMC
- ✧ RG methods: $V_{\text{low } k}$

Phenomenological Approaches

Based on effective density-dependent interactions with parameters adjusted to reproduce nuclear observables & compact star properties.

- ✧ Non-relativistic: Skyrme & Gogny
- ✧ Relativistic: RMF

Non-homogeneous matter

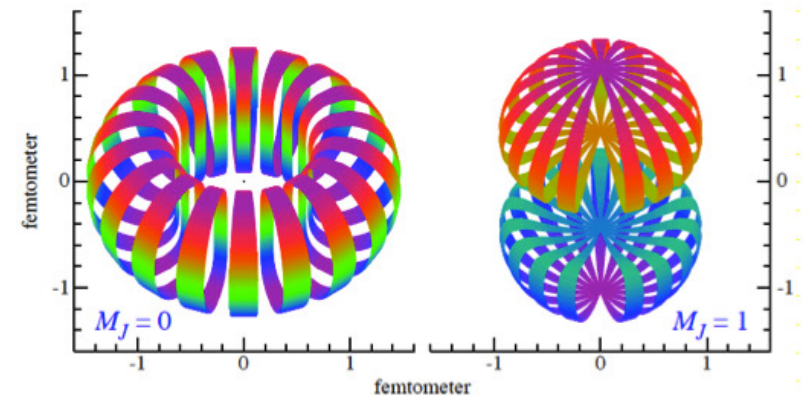
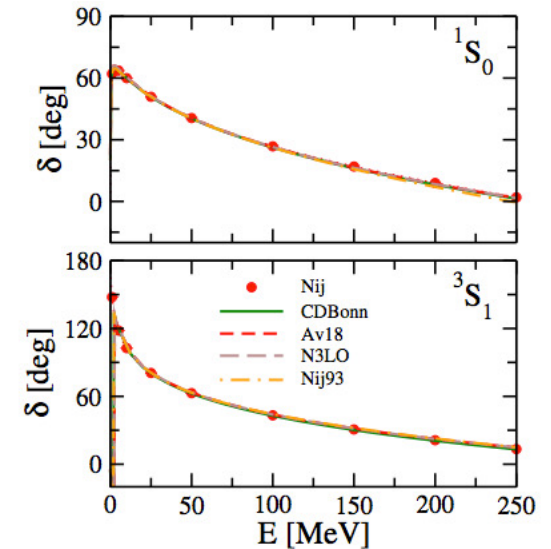
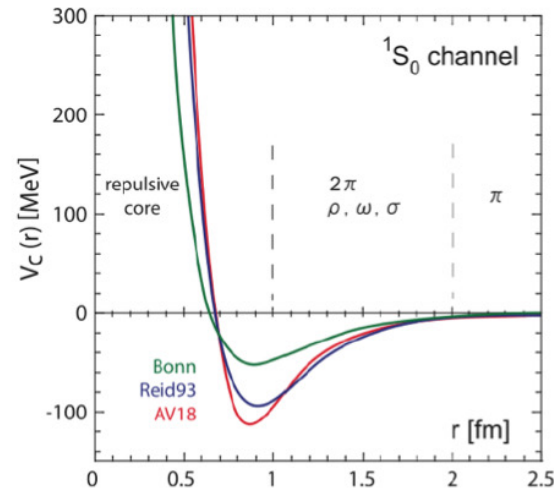
- ✧ SN approximation models: Liquid drop models, TF models, Self-consistent models
- ✧ NSE models: NSE, Virial EoS, models with in-medium mass shifts

Difficulties of ab-initio approaches

✧ Different NN potentials in the market ...
but all are phase-shift equivalent

✧ Short range repulsion makes any
perturbation expansion in terms of V
meaningless. Different ways of treating
SRC

✧ Complicated channel & operatorial
structure (central, spin-spin, spin-
isospin, tensor, spin-orbit, ...)



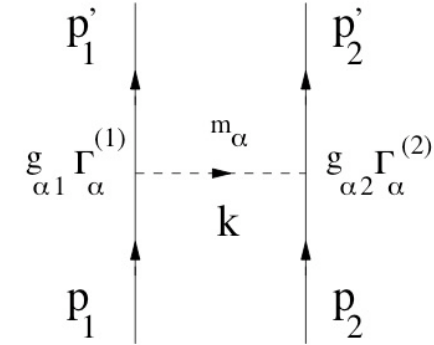
The NN interaction: meson exchange & potential models

✧ Meson Exchange Models:

NN interaction mediated by the **exchange** of different **meson** fields (e.g, Bonn, Nijmegen)

- ✧ scalar: σ, δ $\Gamma_s = 1$
- ✧ pseudoscalar: π, K, η $\Gamma_{ps} = i\gamma^5$
- ✧ vector: ρ, K, ω, ϕ $\Gamma_v = \gamma^\mu, \Gamma_T = \sigma^{\mu\nu}$

$$L = g_M \Gamma_M (\bar{\Psi}_B \Psi_B) \phi_M$$



$$\langle p_1' p_2' | V_M | p_1 p_2 \rangle = \bar{u}(p_1') g_M^{(1)} \Gamma_M^{(1)} u(p_1) \frac{P_M}{(p_1 - p_1')^2 - m_M^2} \bar{u}(p_2') g_M^{(2)} \Gamma_M^{(2)} u(p_2)$$



Machleidt et al., PR. 149, 1 (1987)

Nagels et al., PRD 17, 768 (1978)

✧ Potential Models:

NN interaction is given by the **sum** of several **local operators** (e.g., Urbana, Argonne)

Ex: **Local operators of Av18 potential**

$$V_{ij} = \sum_{p=1,18} V_p(r_{ij}) O_{ij}^p$$

$$O_{ij}^{p=1,14} = \left[1, (\vec{\sigma}_i \cdot \vec{\sigma}_j), S_{ij}, \vec{L} \cdot \vec{S}, L^2, L^2 (\vec{\sigma}_i \cdot \vec{\sigma}_j), (\vec{L} \cdot \vec{S})^2 \right] \otimes [1, (\vec{\tau}_i \cdot \vec{\tau}_j)]$$

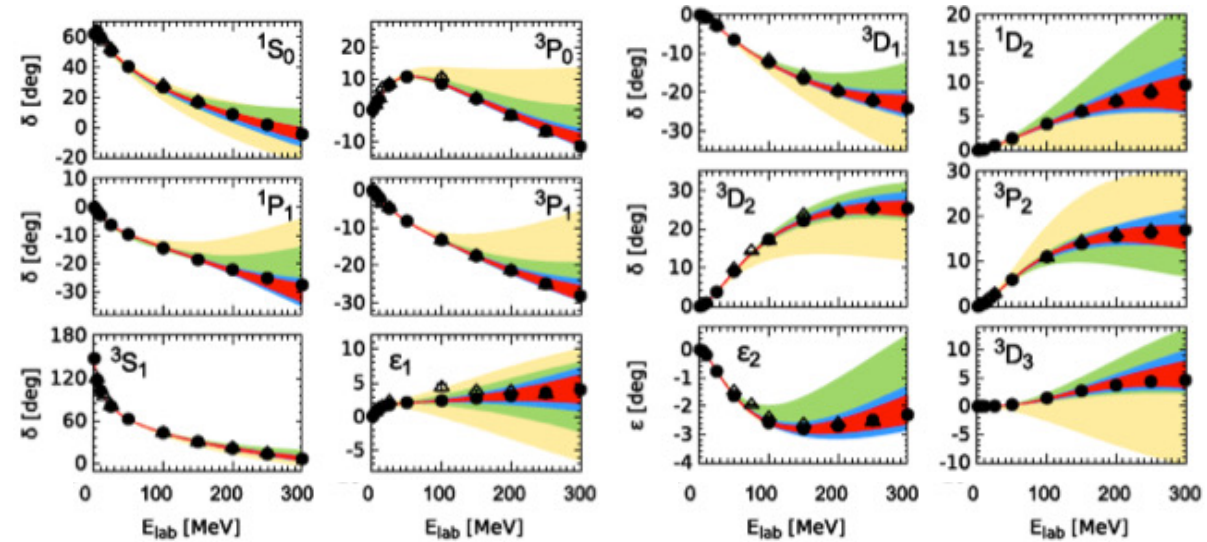
$$O_{ij}^{p=15,18} = [T_{ij}, (\vec{\sigma}_i \cdot \vec{\sigma}_j) T_{ij}, S_{ij} T_{ij}, (\tau_{zi} + \tau_{zj})]$$



Wiringa et al., PRC 51, 38 (1995)

The NN interaction: χ EFT forces

	NN	3N	4N
LO			
NLO			
N ² LO			
N ³ LO			
	+ ...	+ ...	+ ...



- ✧ Starting point: **most general effective chiral Lagrangian** that respect required QCD symmetries where π & N (recently also Δ) are the relevant d.o.f. of the theory
- ✧ **Systematic expansion** in powers of Q/Λ_χ [$Q=m_\pi, k$; $\Lambda_\chi \sim 1$ GeV]
- ✧ **Consistent derivation** of 2N, 3N, 4N, ... forces



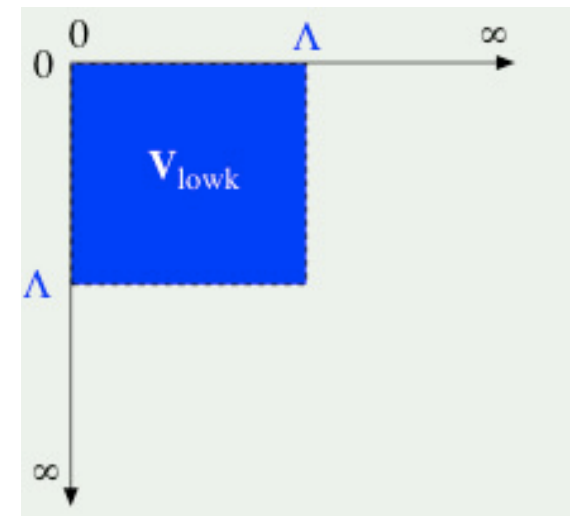
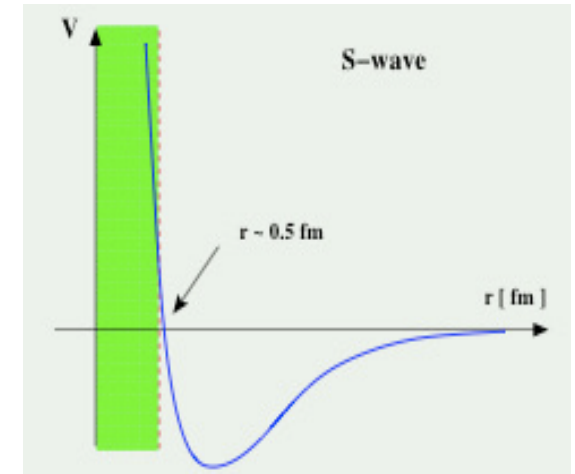
Weinberg, PLB 251, 288 (1990); NPB 363, 3 (1991)
 Entem & Machleidt, PRC 68, 041001(R) (2003)
 Epelbaum et al., NPA 747, 363 (2005)

Renormalization Group Method

- The presence of a short-range hard core of the nucleon-nucleon interaction V makes **any perturbation expansion in terms of V meaningless**
- A possible way to soften it consists in **integrating out all the momenta q larger than a certain cut-off Λ** obtaining in this way effective interaction $V_{low\ k}$ that is equivalent to the original one for momenta $q < \Lambda$

This results in a **modified Lippmann-Schwinger equation** with a cut-off dependent effective potential $V_{low\ k}$

$$T(k', k; E_k) = V_{low\ k}(k', k) + \frac{2}{\pi} P \int_0^{\Lambda} dq q^2 \frac{V_{low\ k}(k', q) T(q, k; E_k)}{k^2 - q^2 + i\eta}$$



Renormalization Group Method

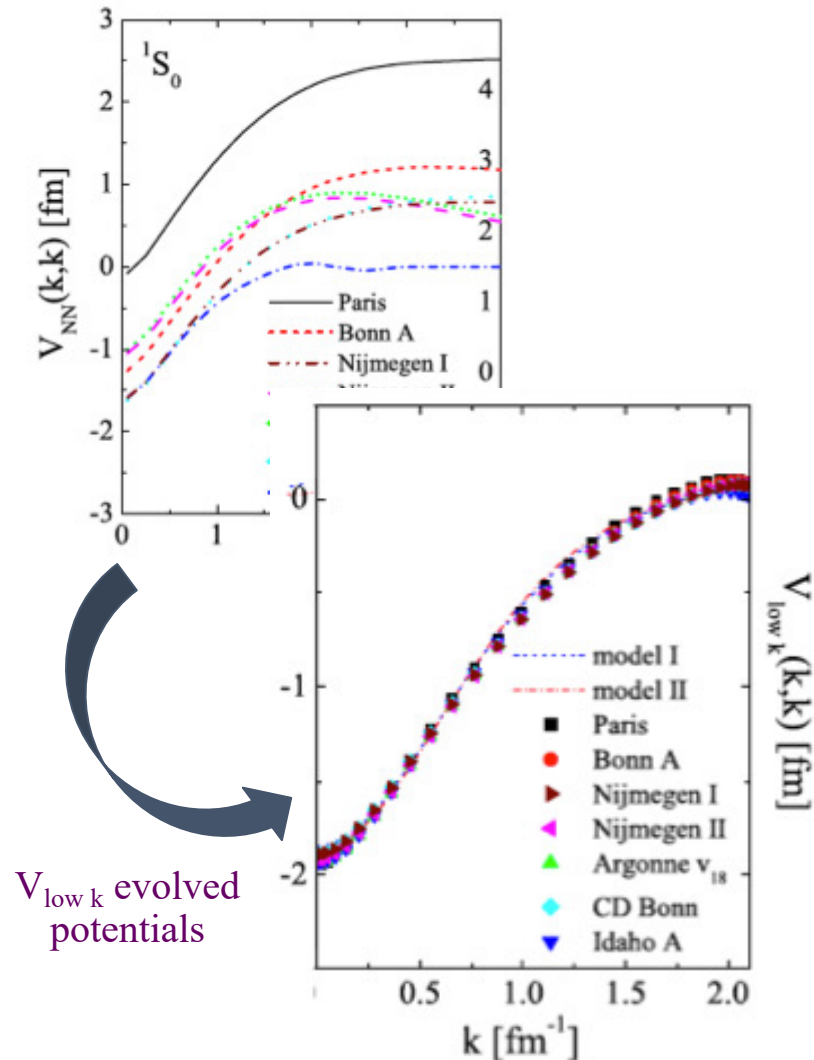
- By demanding $\frac{dT(k',k;E_k)}{d\Lambda} = 0$ one obtains a **Renormalization Group equation** for $V_{low\ k}$

$$\frac{dV_{low\ k}(k',k)}{d\Lambda} = \frac{2}{\pi} \frac{V_{low\ k}(k',k)T(\Lambda, k, \Lambda^2)}{1 - k^2/\Lambda^2}$$

- Integrating this flow equation one obtains a **“universal”** nucleon-nucleon low-momentum potential $V_{low\ k}$ that is:

- ✓ phase shift equivalent
- ✓ energy independent
- ✓ softer (no hard core)
- ✓ hermitian

- Having a much **softer core** the $V_{low\ k}$ potential can be used in **perturbation expansions** and **nuclear structure calculations** in a more efficient way
- The method has been applied also to the hyperon-nucleon case. The results seem to indicate a similar convergence to a **“universal” softer low-momentum hyperon-nucleon interaction**



Baryon-baryon interactions from Lattice QCD

NPLQCD & the HALQCD strategies

➤ NPLQCD

Combines calculations of **correlation functions** of **two-baryon systems** at several light-quark-mass values with **low-energy effective field theory** to extract scattering phase-shifts

➤ HALQCD

- Determine the **Nambu-Bethe-Salpeter wave function** on the lattice

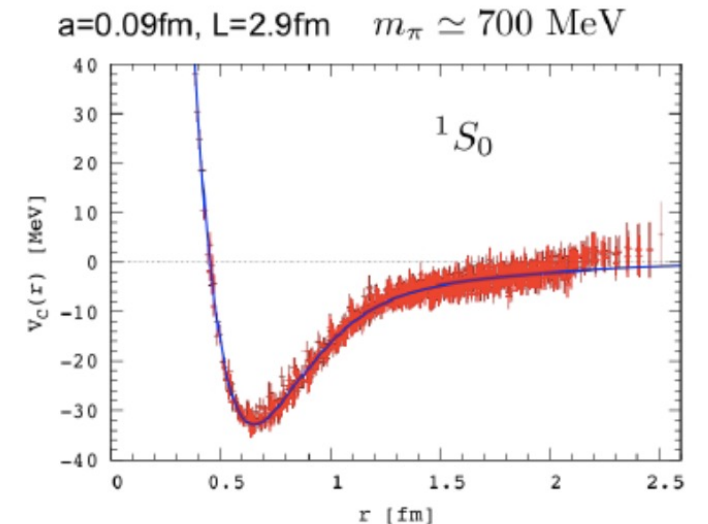
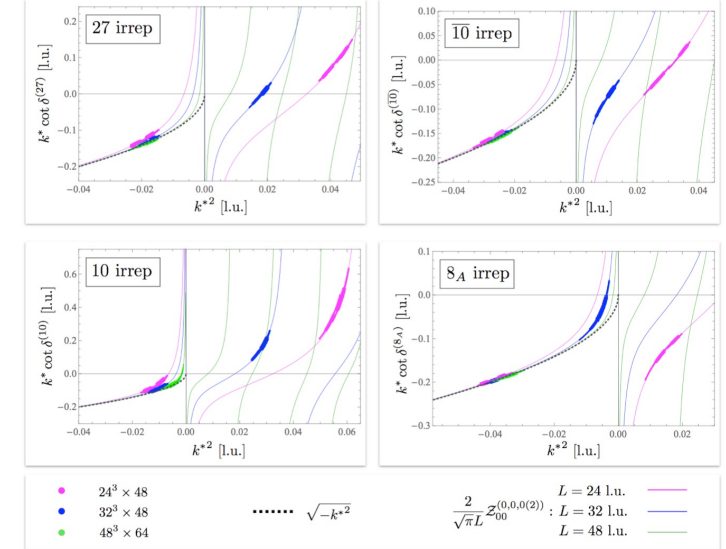
$$\varphi_{E(r)} = \langle 0 | N((x+r, 0) N(x, 0) | 6q, E \rangle, N(x) = \varepsilon_{abc} q^a(x) q^b(x) q^c(x)$$

- Define a **local potential** $U(x, y)$ from $\varphi_{E(r)}$

$$\left[E - \frac{\hbar^2 \nabla^2}{2\mu_N} \right] \varphi_{E(x)} = \int d^3y U(x, y) \varphi_{E(y)}, \quad U(x, y) = V(x, \nabla) \delta(x - y)$$

$$V(x, \nabla) = V_c(x) + V_T(x) S_{12} + V_{LS}(x) \vec{L} \cdot \vec{S} + \{V_D, \nabla^2\} + \dots$$

- Calculate **observables** (phase shifts, binding energies, ...)



Variational & Diagrammatic Approaches

✧ Variational Approach

Based on the **variational principle**

$$E \leq \min \left\{ \frac{\langle \Psi_T | \hat{H} | \Psi_T \rangle}{\langle \Psi_T | \Psi_T \rangle} \right\}, \quad |\Psi_T\rangle = \hat{F} |\Phi\rangle, \quad \hat{F} = \prod_{i>j} \sum_p f^{(p)}(r_{ij}) \hat{O}_{ij}^{(p)}$$

correlation operator uncorrelated w.f.

$f^{(p)}(r_{ij})$ determined through functional minimization of the energy using techniques like **FHNC** or **VMC**



Fantoni & Rosati, Nuov. Cim. 25A, 593 (1975)

✧ SCGF formalism

Energy obtained from the **Galitskii-Migdal-Koltum (GMK)** sum rule

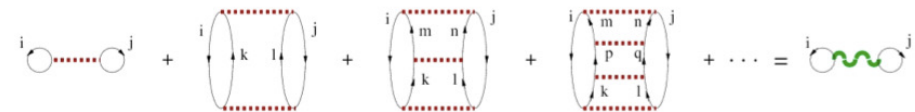
$$E = \frac{v}{\rho} \int \frac{d^3k}{(2\pi)^3} \int_{-\infty}^{\infty} \frac{d\omega}{2\pi} \frac{1}{2} \left\{ \frac{\hbar^2 k^2}{2m} + \omega \right\} A(\vec{k}, \omega) f(\omega)$$

s. p. spectral function

FD distribution

✧ BBG theory

Ground state energy of nuclear matter evaluated in terms of the **hole-line expansion** derived by means of **Brueckner reaction matrix**



BHF:

$$E_{BHF} = \sum_{i \in A} \langle \alpha_i | K | \alpha_i \rangle + \frac{1}{2} \text{Re} \left[\sum_{i, j \in A} \langle \alpha_i \alpha_j | G(\omega) | \alpha_i \alpha_j \rangle \right]$$



Day, RMF.39, 719 (1967)

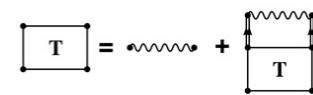


Infinite summation of **two-hole line** diagrams

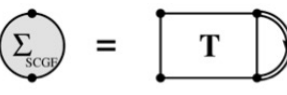
Spectral function

$$A(\vec{k}, \omega) = \frac{-2 \text{Im} \Sigma(\vec{k}, \omega)}{\left[\omega - \frac{\hbar^2 k^2}{2m} - \text{Re} \Sigma(\vec{k}, \omega) \right]^2 + [\text{Im} \Sigma(\vec{k}, \omega)]^2}$$

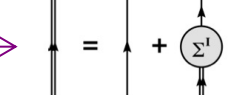
In-medium interaction



Ladder self-energy



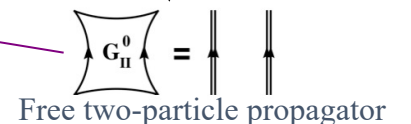
Dyson equation



Self-consistent scheme



Carbone et al, PRC 88, 054326 (2013)



Free two-particle propagator

Quantum Monte-Carlo Techniques

✧ VMC:

Evaluate energy & other observables using the **Metropolis algorithm**

$$\langle \hat{O} \rangle = \frac{\sum_i \langle \Psi(\vec{R}_i) | \hat{O} | \Psi(\vec{R}_i) \rangle / W(\vec{R}_i)}{\sum_i \langle \Psi(\vec{R}_i) | \Psi(\vec{R}_i) \rangle / W(\vec{R}_i)}$$



Wiringa et al., PRC 62, 014001 (2000)

✧ DMC:

Model a diffusion process rewriting the **Schoedinger** equation in **imaginary time**

$$i \frac{\partial}{\partial t} |\Psi\rangle = \hat{H} |\Psi\rangle \Rightarrow -\frac{\partial}{\partial \tau} |\Psi\rangle = \hat{H} |\Psi\rangle$$



Anderson, J. Chem. Phys. 63, 1499 (1975)

✧ GFMC:

Sample a **trial wave function** by evaluating **path integrals** of the form

$$|\Psi(\tau)\rangle = \prod \exp\left[-(\hat{H} - E_0)\Delta\tau\right] |\Psi_v\rangle$$
$$|\Psi(\tau)\rangle \xrightarrow{n \rightarrow \infty} |\Psi_0\rangle$$



Carlson et al., PRC 68, 025802 (2003)

✧ AFDMC:

Rewrite Green's function in order to change the quadratic dependence on spin & isospin operators to a linear one by introducing **Hubbard-Stratonovich auxiliary fields**



Gandolfi et al., PRC 79, 054005 (2009)

Phenomenological Models: Skyrme & Gogny interactions

✧ Skyrme interactions:

Effective **zero-range** density dependent interaction

$$\begin{aligned}\hat{V}(\vec{r}_1, \vec{r}_2) = & t_0 \left(1 + x_0 \hat{P}_\sigma\right) \delta(\vec{r}_{12}) + \frac{t_1}{2} \left(1 + x_1 \hat{P}_\sigma\right) \left[\hat{k}' \delta(\vec{r}_{12}) + \delta(\vec{r}_{12}) \hat{k}^2 \right] \\ & + t_2 \left(1 + x_2 \hat{P}_\sigma\right) \hat{k}' \delta(\vec{r}_{12}) \hat{k} + \frac{t_3}{6} \left(1 + x_3 \hat{P}_\sigma\right) \rho^\alpha(\vec{R}_{12}) \delta(\vec{r}_{12}) \\ & + i W_0 \left(\hat{\sigma}_1 + \hat{\sigma}_2\right) \left[\hat{k}' \times \delta(\vec{r}_{12}) \hat{k} \right]\end{aligned}$$



Evaluation of the energy density in the **HF approximation** yields for nuclear matter a simple EDF in **fractional powers of the number densities**. Many parametrizations exist



Skyrme, Nucl. Phys. 9, 615 (1959)

✧ Gogny interactions:

Effective **finite-range** density dependent interaction

$$\begin{aligned}\hat{V}(\vec{r}_1, \vec{r}_2) = & \sum_{j=1,2} \exp\left(-\frac{r_{12}^2}{\mu_j^2}\right) \left(W_j + B_j \hat{P}_\sigma - H_j \hat{P}_\tau - M_j \hat{P}_\sigma \hat{P}_\tau \right) \\ & + t_0 \left(1 + x_0 \hat{P}_\sigma\right) \rho^\alpha(\vec{R}_{12}) \delta(\vec{r}_{12}) \\ & + i W_0 \left(\hat{\sigma}_1 + \hat{\sigma}_2\right) \left[\hat{k}' \times \delta(\vec{r}_{12}) \hat{k} \right]\end{aligned}$$



Due to the **finite-range** terms the evaluation of the energy density is **numerically more involved**. Less number of parametrizations in the market



Brink & Boeker, NPA 91, 1 (1967)

Phenomenological Models: Relativistic Mean Field Models

Based in **effective Lagrangian densities** where the interaction is modeled by **meson exchanges**

$$L = L_{nuc} + L_{mes} + L_{int} + L_{nl}$$

$$L_{nuc} = \sum_{i=n,p} \bar{\psi}_i (\gamma_\mu i\partial^\mu - m_i) \psi_i$$

$$L_{mes} = \frac{1}{2} (\partial^\mu \sigma \partial_\mu \sigma - m_\sigma^2) + \frac{1}{2} (\partial^\mu \vec{\delta} \partial_\mu \vec{\delta} - m_\sigma^2) - \frac{1}{4} G_{\mu\nu} G^{\mu\nu} + \frac{1}{2} m_\omega^2 \omega_\mu \omega^\mu - \frac{1}{4} H_{\mu\nu} H^{\mu\nu} + \frac{1}{2} m_\omega^2 \vec{\rho}_\mu \cdot \vec{\rho}^\mu$$

$$L_{int} = - \sum_{i=n,p} \bar{\psi}_i \left[\gamma_\mu (g_\omega \omega^\mu + g_\rho \vec{\tau} \cdot \vec{\rho}^\mu) + g_\sigma \sigma + g_\delta \vec{\tau} \cdot \vec{\delta} \right] \psi_i$$

$$L_{nl} = -\frac{A}{3} \sigma^3 - \frac{B}{4} \sigma^4 + \frac{C}{4} (\omega_\mu \omega^\mu)^2 + D (\omega_\mu \omega^\mu) (\vec{\rho}_\mu \cdot \vec{\rho}^\mu)$$

Nucleon & meson equations of motion are derived from the Lagrangian density and usually self-consistently solved in the **mean field approximation** where mesons are treated as **classical fields** and **negative-energy states** of baryons are **neglected**



Boguta & Bodmer, NPA 292, 413 (1977)

Serot & Walecka, Adv. Nuc. Phys. 16, 1 (1986)

EoS for non-homogeneous nuclear matter

Non-uniform nuclear matter is present in the **NS crust and SN cores** (low ρ , low T). Till now only **two types of phenomenological approaches** have been used to describe it:

Single-nucleus approximation models

Composition of matter is assumed to be made of **one representative heavy nucleus** (the one energetically favored) + light nuclei (α particles) or unbound nucleons

- ✓ (Compressible) Liquid-Drop models
- ✓ (Extended) Thomas-Fermi models
- ✓ Self-consistent mean-field models

Nuclear Statistical Equilibrium models

Composition of matter is assumed to be a **statistical ensemble** of different nuclear species and nucleons in thermodynamical equilibrium

- ✓ (Extended) NSE
- ✓ Virial EoS
- ✓ Models with in-medium mass shifts

The final message of this talk



The Nuclear EoS is a fundamental ingredient for the understanding of the static & dynamical properties of NS, core-collapse SN & compact star mergers

- ✧ Major experimental, observational & theoretical advances on understanding the nuclear EoS have been done in the last decades & will be done in the near future
- ✧ The isoscalar part of the nuclear EoS is rather well constrained
- ✧ Why the isovector part is less well constrained is still an open question whose answer is probably related to our limited knowledge of the nuclear force and, particularly, of its spin & isospin dependence

- ✧ You for your time & attention
- ✧ The organizers for their kind invitation & support

